

Optimization of self-coherent reflective PON to achieve a new record 42 dB ODN power budget after 100 km at 1.25 Gbps

S. Straullu,^{1,*} F. Forghieri,³ V. Ferrero,² and R. Gaudino²

¹ISMB, Istituto Superiore Mario Boella, Via P.C. Boggio 61—10138 Torino, Italy

²Politecnico di Torino, C.so Duca degli Abruzzi 24—10129 Torino, Italy

³CISCO Photonics, Via Philips 12, 20059, Monza, Milan, Italy

*straullu@ismb.it

Abstract: We demonstrate a greater than 42 dB optical distribution network power budget in the upstream of a 1.25 Gbps self-coherent reflective PON after 100 km of installed fibers, using off-the-shelf optoelectronic components, improving our previous result by 4 dB. We discuss all system optimizations introduced in the setup in order to reach such a result, including 8B/10B high-pass filtering and Faraday rotation at the ONU.

©2012 Optical Society of America

OCIS codes: (060.0060) Fiber optics and optical communications; (060.1660) Coherent communications; (060.4080) Modulation.

References and links

1. S. P. Jung, Y. Takushima, and Y. C. Chung, "Transmission of 1.25-Gb/s PSK signal generated by using RSOA in 110-km coherent WDM PON," *Opt. Express* **18**(14), 14871–14877 (2010).
 2. I. Papagiannakis, M. Omella, D. Klonidis, J. A. Lázaro Villa, A. N. Birbas, J. Kikidis, I. Tomkos, and J. Prat, "Design characteristics for a full-duplex IM/IM bidirectional transmission at 10 Gb/s using low bandwidth RSOA," *J. Lightwave Technol.* **28**(7), 1094–1101 (2010).
 3. K. Y. Cho, Y. Takushima, and Y. C. Chung, "10-Gb/s operation of RSOA for WDM PON," *IEEE Photon. Technol. Lett.* **20**(18), 1533–1535 (2008).
 4. Y. Takushima, K. Y. Cho, and Y. C. Chung, "Design issues in RSOA-based WDM PON," in *IEEE PhotonicsGlobal@Singapore, 2008. IPGC 2008* (IEEE, 2008), pp. C-34–C-37.
 5. B. Charbonnier, A. Lebreton, S. Straullu, V. Ferrero, A. Sanna, and R. Gaudino, "Self-coherent single wavelength SC-FDMA PON uplink for NG-PON2," in *Optical Fiber Communication Conference, OSA Technical Digest* (Optical Society of America, 2012), paper OW4B.4.
 6. Y. Luo, X. Zhou, F. Effenberg, X. Yan, G. Peng, Y. Qian, and Y. Ma, "Time and wavelength division multiplexed passive optical network (TWDM-PON) for next generation PON stage 2 (NG-PON2)," *J. Lightwave Technol.*, to be published.
 7. K. Y. Cho, K. Tanaka, T. Sano, S. P. Jung, J. H. Chang, Y. Takushima, A. Agata, Y. Horiuchi, M. Suzuki, and Y. C. Chung, "Long-reach coherent WDM PON employing self-polarization-stabilization technique," *J. Lightwave Technol.* **29**(4), 456–462 (2011).
 8. G. Rizzelli, V. Ferrero, S. Straullu, S. Abrate, F. Forghieri, and R. Gaudino "Record-high ODN power budget (more than 38 dB) in self-coherent reflective PON at 1.25 Gbit/s after propagation through 80 km installed fibers," in *European Conference and Exhibition on Optical Communication, OSA Technical Digest* (online) (Optical Society of America, 2012), paper We.1.B.3.
 9. International Telecommunication Union, ITU-T Recommendation G.984.2 (2003) Amendment 2 (03/08).
 10. G. Rizzelli, V. Ferrero, S. Straullu, S. Abrate, F. Forghieri, and R. Gaudino "Optimization of uncooled RSOA parameters in WDM reflective PONs based on self-coherent or direct detection OLT receivers," in *European Conference and Exhibition on Optical Communication, OSA Technical Digest* (online) (Optical Society of America, 2012), paper We.1.B.1.
 11. M. O. Van Deventer, "Polarization properties of Rayleigh backscattering in single-mode fibers," *J. Lightwave Technol.* **11**(12), 1895–1899 (1993).
 12. S. J. Savory, "Digital filters for coherent optical receivers," *Opt. Express* **16**(2), 804–817 (2008).
 13. E. K. MacHale, G. Talli, P. D. Townsend, A. Borghesani, I. Lealman, D. G. Moodie, and D. W. Smith, "Signal-induced Rayleigh noise reduction using gain saturation in an integrated R-EAM-SOA," in *Optical Fiber Communication Conference, OSA Technical Digest* (CD) (Optical Society of America, 2009), paper OThA6.
 14. C. R. Doerr, L. L. Buhl, Y. Baeyens, R. Aroca, S. Chandrasekhar, X. Liu, L. Chen, and Y. K. Chen, "Packaged monolithic silicon 112-Gb/s coherent receiver," *IEEE Photon. Technol. Lett.* **23**(12), 762–764 (2011).
-

1. Introduction

In WDM-PON research, there has recently been a vast amount of work on reflective ONU solutions [1–5] that allow us to avoid tunable lasers at the ONU to target colorless and inexpensive RSOA-based ONUs. Most of these solutions have a limited optical distribution network (ODN) power budget in the upstream path (denoted “max ODN loss” in the rest of this paper), which is a key parameter in extended reach PONs and/or in WDM-PONs that use optical filters not in the ODN, but only at the ONU and OLT, thus retaining the splitter-based ODN. This is the favorite choice for most telecom operators, as was also clearly pointed out by the recent FSAN decision for the NG-PON2 architecture, which will be TWDM and splitter-based [6] and will thus require at least the same ODN power budget as the previous standards GPON and XGPON (such as 28 dB for GPON class B+ and 32 dB for class C+).

In order to overcome the reflective-PON power budget limitation, it was recently shown [7,8] that self-coherent detection on the upstream can greatly increase max ODN loss. For instance, in our ECOC 2012 paper [8], a 38 dB ODN loss over 80 km at 1 Gbps was seen. In the present paper our previous results have been improved to more than 42 dB (for $\text{BER} = 10^{-3}$) over a longer distance of 100 km, after a careful optimization of several system parameters. This result, obtained by using real metropolitan buried fibers and off-the-shelf optoelectronic components for the TX/RX hardware, shows the potential compatibility even with a GPON class C+ ODN loss target (32 dB) [9], offering a huge 10 dB margin that can largely cope with TX-RX thermal [10] and ageing effects, not addressed in this paper but obviously very relevant in real-life outdoor FTTH installations. The rationale and novelty of the present paper consists in the following main points:

- Demonstration of the aforementioned 42 dB ODN loss and its verification over long-term repeated measurements;
- Detailed presentation of the physical layer effects that affect this specific system, in particular Rayleigh back-scattering (RBS) and its dependence on polarization;
- A description of all the hardware and digital signal processing (DSP) techniques introduced to overcome RBS impairments.

The paper is organized as follows: in Section 2 the experimental setup is described; then in Section 3 the results in the different configurations are presented. Finally, in Section 4, several points related to DSP optimization, Faraday rotation at the ONU, and the rationale for the high ODN optical power budget are discussed.

We stress that the paper is intentionally focused on ODN loss margins on the upstream path as a fundamental parameter to assess the quality of the proposed system and that the experiments have been performed on a real installed buried SMF fiber, organized in a worst-case configuration from the Rayleigh back-scattering (RBS, see Section 2) impairment point of view, one of the key limiting physical effects in these types of architecture.

2. Experimental setup

The system setup is shown in Fig. 1. It emulates the upstream path of a long-reach, high ODN loss PON. At the OLT side, a CW laser (external cavity, 1550.92 nm) is used both as a feed to be sent downstream to the RSOA (ONU side) and as a local oscillator for the OLT coherent receiver (Neophotonics, back-to-back sensitivity equal to -52.5 dBm for $\text{BER} = 10^{-3}$, line rate 1.25 Gbps). The OLT is linked to the ODN by either a circulator (indicated as “standard” setup in the following, shown in Fig. 1(a)) or a polarizing beam splitter (“Faraday” setup shown in Fig. 1(b) [7,8]). The ODN uses 100 km of SMF buried metropolitan fiber running around the Turin (Italy) city center and terminated in our labs. The fiber is quite old, deployed underground between 1990 and 2000, characterized by high attenuation and several connectors and splices along the path. Its overall attenuation over 100 km is equal to 32 dB. (For the G.652 fiber at the C-band only, the PMD values were between approximately 0.082

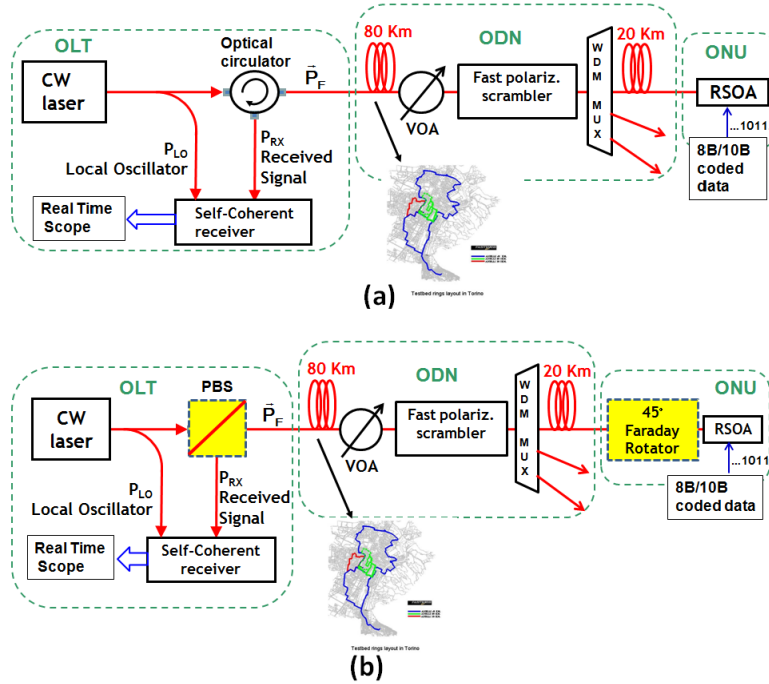


Fig. 1. Experimental setup, (a) “Standard” architecture and (b) “Faraday” architecture.

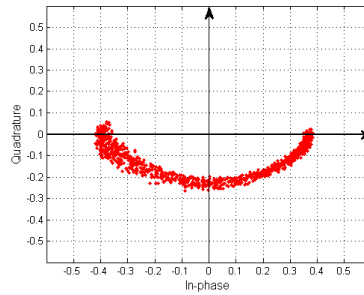


Fig. 2. Scattering diagram for the quasi BPSK modulation at the output of the RSOA (parameters $P_F = 0$ dBm, $I_b = 75$ mA, $V_{pp} = 1.5$ V).

and 0.136 ps/km^2). In both architectures, in addition to the fiber, the ODN path was composed by the following:

- An arrayed waveguide gratings (AWG), to manage multiple optical wavelengths;
- A variable optical attenuator (VOA), to increase ODN loss for BER measurements (to emulate a worst-case situation in terms of reflections, inserted after 80 km of fiber, before the AWG);
- A fast polarization scrambler (PS, implementing full rotations on the Poincaré sphere in less than 3 ms), set in continuously changing mode to emulate random fiber birefringence. This device was necessary because polarization changes deeply affect the performance of our system (see below).

The ONU is constituted by an uncooled low cost RSOA (Kamelian, TO-Can package). The RSOA input parameters (peak-to-peak modulation voltage V_{pp} and bias current I_b) have

been changed to evaluate the maximum ODN loss (L_{ODN}) to get $BER \leq 10^{-3}$ as in [10]. The optimized values were $I_b = 75$ mA and $V_{pp} = 1.5$ V, which quite interestingly do not generate an On-Off modulation, but conform to a “quasi” BPSK modulation format as shown in the scattering diagram of Fig. 2 [10], i.e., to a phase modulated signal (thanks to the RSOA chirp). For the “Faraday” setup of Fig. 1(b), a 45° Faraday rotator (FR) was also inserted in front of the RSOA, so that the polarization of the reflected (and modulated) signal is always orthogonal to the incoming one thanks to the two 45° Faraday rotations. Because of fiber reciprocity, it can be shown that the polarization orthogonality between the upstream and the downstream signals is preserved in any ODN path section, regardless of fiber birefringence [11]. In both architectures, the resulting BER was evaluated by off-line processing. On the OLT side, for self-coherent detection operations, quite common digital signal processing (DSP) techniques (such as carrier-phase Viterbi-Viterbi estimation and LMS adaptive equalization [12]) are currently being used.

3. Experimental results

In Fig. 3(a) is shown, for the “Faraday” setup, the BER vs. ODN loss after 100 km for various launched power values from +6 to +11 dBm at the OLT output (P_F). Each dot in the graphs gives the BER evaluated in off-line processing over approximately 2×10^5 bits. For each condition, 20 BER measurements (reported in the graph) were repeated while continuously varying the ODN birefringence. The solid curves connect the median of each set of 20 BER values. The graph demonstrates that our system can tolerate more than 42 dB of ODN loss (at $BER = 10^{-3}$) for P_F above +9 dBm. The same measurements are also shown in Fig. 3(b) for the “standard” setup, which, compared with the Faraday setup, shows an approximately 2 dB penalty (at $BER = 10^{-3}$) for $P_F = 10$ dBm and shows the onset of nonlinearities for $P_F = 11$ dBm.

Figures 4(a) and 4(b) represent the results of a very long set of repeated measurements (1000 acquisition over 8 hours) for the “Faraday” and “standard” setups, respectively. In both cases the long time measurements do not show any “out of service” point (at $BER = 0.5$), demonstrating the excellence of the reflective PON architecture. Moreover, the “Faraday” setup shows better stability in the obtained BER values than in the “standard” setup.

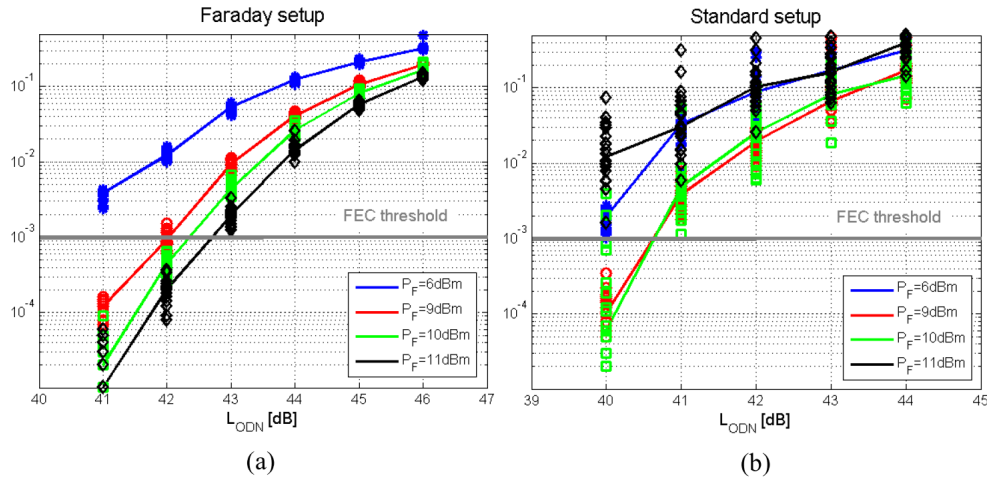


Fig. 3. BER vs. L_{ODN} for (a) the “Faraday” and (b) “standard” setup using various launched powers P_F .

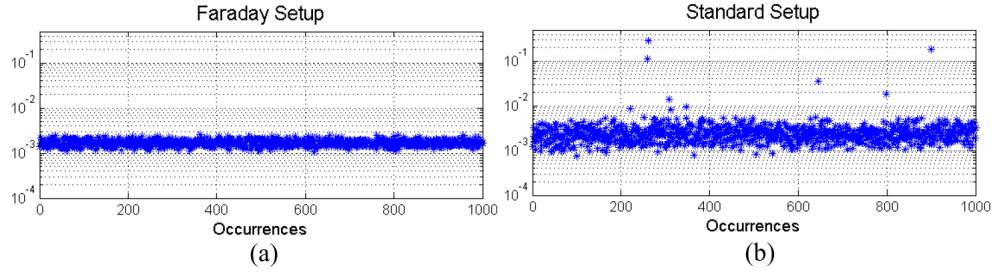


Fig. 4. Repeated measurements for (a) the “Faraday” setup ($L_{ODN} = 42.1$ dB) and (b) the “standard” setup ($L_{ODN} = 40.5$ dB), $P_F = 9$ dBm, 100 km.

4. Discussion on experimental results and system optimization in DSP and hardware

Performing simple power budget calculus, it is possible to observe that

- The received power at the OLT self-coherent receiver is $P_{RX} = P_F - 2 \cdot L_{ODN} + G_{RSOA}$, where L_{ODN} is the ODN loss and $G_{RSOA} \cong 24$ dB is the RSOA round-trip gain. For instance, for $P_F = 9$ dBm and $L_{ODN} = 42$ dB, the value $P_{RX} = -51$ dBm is obtained.
- The spurious signal generated by concentrated and RBS reflections on the downstream CW can be estimated as $P_{refl} = P_F - R_{ODN}$, where R_{ODN} is the ODN backreflection value, typically in the 30–35 dB range (GPON ITU-T Recommendation [9]). For instance, for $L_{ODN} = 42$ dB and $R_{ODN} = 35$ dB, the spurious signal turns out to be 25 dB higher than the useful received signal, and spectrally is totally superimposed.

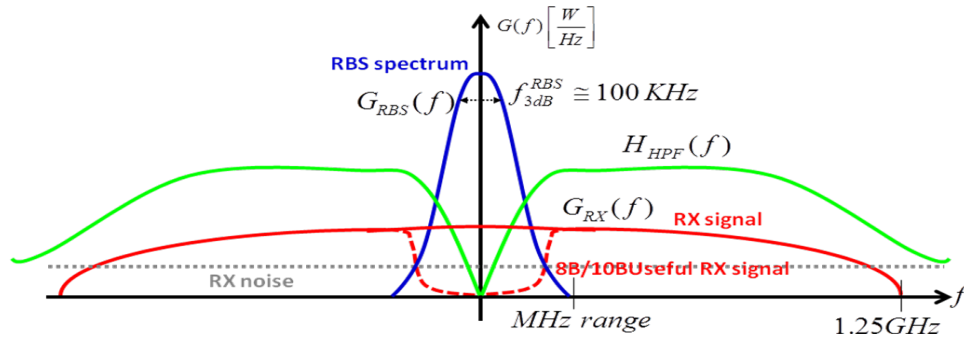


Fig. 5. Qualitative representation of relevant signals at the output of the self-coherent receiver in the frequency domain (power spectrum). Blue curve, RBS component; solid red curve, uncoded modulated signal; dashed red curve, 8B/10B coded signal; green curve, high-pass filter.

The useful signal and the spurious RBS power levels calculated above drove the optimization that has been performed in the system. First, just by looking at the required sensitivity (about -51 dBm), it becomes obvious that a coherent receiver is a must. However, its importance goes significantly further: because of the presence of a RBS [11] crosstalk component that is much stronger than the useful signal, a direct-detection receiver would simply not work, owing to the beating accompanying a CW signal. Many research groups have addressed the topic of reducing the effect of RBS in direct-detection receivers by using different optical or electrical techniques, but, to the best of our knowledge, none can function with an optical signal to Rayleigh noise ratio (OSNRN) lower than 5–6 dB [13], while here the OSNRN target was in the negative range, such as the previously discussed -25 dB OSNRN value. The self-coherent receiver is key here, since it provides access in the electrical

domain to an exact replica of the received optical field (and not just its instantaneous power, as in direct detection) such that there is no beating between the signal and the RBS, but the two signals simply appear as added, both at the field level and in the equivalent electrical components after coherent detection. To clarify the situation, in Fig. 5 we show a qualitative representation of the just discussed relevant signals as seen at the coherent receiver output in the electrical domain, since this representation will be useful to explain some of the considerations that follow. As shown in Fig. 5, the RBS spectrum appears after coherent detection as low-frequency components around $f = 0$, and it has a shape that depends only on the CW external cavity laser linewidth Δf_{FWHM} (approximately 100 kHz in our case) and thus appears as narrow band when compared with the modulated useful signal, but is much stronger in amplitude, since the OSNR reference target is negative. The useful modulated signal is also centered around $f = 0$, but with a much broader spectrum. To spectrally reject the RBS, the solution was to perform a high-pass filtering (HPF) in the coherent receiver (shown as a green curve in Fig. 5), in order to cut the DC-like crosstalk interference, optimizing its cut-off frequency f_{HPF} . Since this HPF also affects the useful signal low-frequency components (the continuous red curve of Fig. 5), f_{HPF} choice should balance crosstalk reduction and baseline wandering on the useful signal. Thus an 8B/10B line coding is introduced at the transmitter side that, thanks to the very strong DC-balancing characteristics, generates a strong notch in the signal spectrum at low frequency (represented by the red dashed curve in Fig. 5); so it is possible to significantly increase the HPF frequency cutoff compared with the uncoded modulation, finding an optimized value at around 50 MHz (for a line bit rate equal to 1.25 Gbps after line coding). Initially, this filter was implemented only in the DSP domain, but the results were still unsatisfactory. The culprit was related to quantization problems in the coherent receiver ADC converters (about 7 effective bits in our case), where the ADC dynamic has to be adapted to the full received signal (useful + crosstalk). Since in our target situation the useful signal can even be 25 dB lower than the crosstalk, the ADC dynamic was saturated by the crosstalk, leaving a very limited dynamic (i.e., ADC effective quantization bits) for the useful signal, as shown in Fig. 6(a). The solution was to split the HPF into two parts: a first hardware electrical filter placed before the ADC, to cut a first significant part of the crosstalk spectral components and thus greatly reducing ADC saturation, and a second (more refined) filter implemented in the DSP domain (Fig. 6(b)). The combination of 8B/10B line coding and HPF optimization is the main upgrade of this paper's setup compared with the previous one [8].

Another novelty in this paper was related to the following observations:

- Polarization/birefringence effects in the fiber are very relevant in our system. It was demonstrated [11] that RBS tends to be (statistically) copolarized with the counterpropagating signal that generates it. In the present setup, this means that the RBS is mostly copolarized with the CW feed signal. In contrast, the useful signal (in the “standard” setup) arrives in general at the coherent receiver with an arbitrary polarization, due to random fiber birefringence. The crosstalk system effect is maximum when these two polarizations are aligned, while it is null for a coherent receiver when they are orthogonal.
- Typical off-line processing experiments can capture only a very small time window over each BER measurement, corresponding in our case to approximately 100 μ s.
- “Natural” birefringence variations are very slow even in long fibers, so that our 100 μ s off-line BER measurement is basically instantaneous compared with birefringence time constants.

To rigorously assess the performance of our system, many repeated BER measurements were performed while changing the ODN birefringence using a fast polarization scrambler (PS) placed in the vicinity of the ONU. When using the “standard” setup (i.e., no Faraday rotation at the ONU) it was experimentally found that at high L_{ODN} each set of repeated BER measurements has a significant spread of values, as shown in Fig. 4.

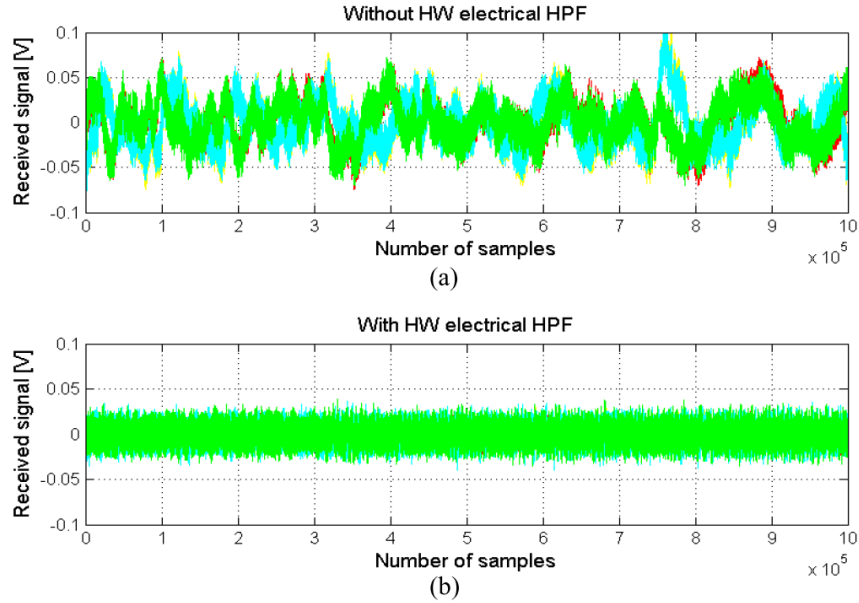


Fig. 6. Received signals acquired (a) without and (b) with the HW electrical HPF (yellow, in-phase component, X polarized; red, quadrature component, X polarized; light-blue, in-phase component, Y polarized; green, quadrature component, Y polarized).

These results have been interpreted as follows: for each individual BER measurement, the useful and crosstalk relative polarization states are changed by the PS, and consequently the resulting BER will be different. Even though the aforementioned HPF + 8B/10B countermeasure greatly diminishes the crosstalk effect, an extreme situation can be observed in which the residual crosstalk after HPF still has some effect on BER, which thus shows a residual dependence on polarization. The situation is significantly different when the “Faraday” setup is used, since the received useful signal polarization at the input of the OLT is always orthogonal to the downstream CW feed signal. As a result, the useful signal tends to be statistically orthogonal to the crosstalk, and thus crosstalk’s effect is minimized. In this way, it is possible to understand why the “Faraday” setup shows better stability in the obtained BER values (see Fig. 4(a)) compared with the “standard” setup performance results of Fig. 4(b).

By optimization of the RSOA driving parameters, combined with a quasi BPSK modulation format (see Fig. 2), RBS rejection, and the use of self-coherent detection, we have demonstrated up to 40 dB ODN losses for the “standard” architecture (Fig. 1(a)), and even 42 dB for the “Faraday” architecture (Fig. 1(b)). The results are summarized in Fig. 7, which shows the achievable ODN loss for $\text{BER} = 10^{-3}$ as a function of the CW power launched by the OLT. For the “Faraday” setup, it is interesting to note that the penalty compared with back-to-back sensitivity is very small (less than 0.5 dB) showing that, thanks to the receiver optimizations previously discussed, the RBS does not greatly affect the performance.

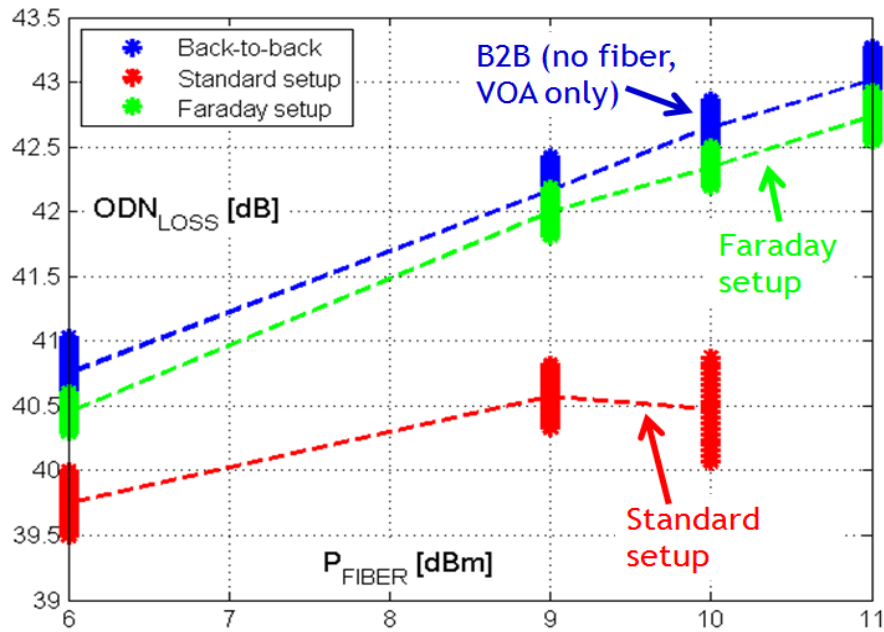


Fig. 7. ODN loss vs. OLT launched power at $\text{BER} = 10^{-3}$.

5. Conclusions

The optimized reflective PON architecture has shown that even for reflective-ONU it is possible to reach very high L_{ODN} , provided RBS crosstalk is properly handled by coherent detection coupled with the following techniques:

- 8B/10B line coding on the RSOA input signal;
- Optimized HPF at the coherent receiver, split in two sections (a simple analogue electrical HPF followed by a digital FIR);
- Faraday rotation at the ONU.

In terms of system cost and the complexity of these three countermeasures, it has been observed that HPF is irrelevant, since cut-off capacitors are almost always present in optical front-ends, and is just needed to decrease their value to obtain a higher cutoff frequency (which usually facilitates the design of the receiver optoelectronic circuits). Also, line coding using 8B/10B does not add significant complexity at the DSP level, apart from the well-known 25% increase in line rate. The implementation of Faraday rotation, in contrast, has a cost related to an additional optical component at the ONU side, but it can be greatly reduced by proposing an integration between the Faraday rotator and the RSOA in the same packaging. Anyway, it has been shown in Fig. 7 that the Faraday setup gives a 2 dB advantage compared with the “standard” setup in terms of L_{ODN} and a smaller spread of the repeated BER measurements, demonstrating the usefulness of the “Faraday” setup. An actual choice between the two options would depend on the system targets, but it is worth mentioning that, even if one decides to stick with the simpler “standard” setup, the achievable L_{ODN} values are still of the order of 40 dB, much better than all results presented so far for reflective PONs.

To end the brainstorming about costs, our key proposal can be summarized as follows:

- The ONU (at least in the “standard” setup) is really extremely simple (RSOA based, uncooled, binary signaling without any requirements in terms of digital signal processing apart from 8B/10B), to such a degree that its cost is expected to be

smaller than, for instance, that of the tunable laser required by the forthcoming NGPON2 TWDM standard [6];

- The OLT, in contrast, is much more expensive than those used so far, because of the presence of a coherent receiver. Will coherent receivers whose cost is compatible with the access network constraints be feasible sooner or later? It is hard to say today, but it is possible to observe that coherent receivers on Silicon Photonics platforms have already been demonstrated [14], showing a roadmap for great cost reduction in the near future.

Acknowledgments

The authors would like to thank Fastweb for allowing the access to their Turin dark fiber metro network and Silvio Abrate of ISMB Istituto Superiore Mario Boella for supporting the experiment.